Free Convection from an Elliptic Tube with its Major Axis Vertical and Placed in a Micropolar Fluid

F. M. MAHFOUZ
Mechanical Department, UET, Taxila, Pakistan,
On leave from Menoufia University, Egypt

Abstract: - In this paper free convection from a horizontal isothermal elliptic tube placed in a micropolar fluid with its major axis vertical is investigated. The governing equations are based on the conservation of mass, linear momentum, angular momentum and energy. The full governing equations written in stream function-vorticity formulation are solved numerically using the Spectral method based on Fourier series expansion. Beside the classical controlling parameters (Rayleigh number, Prandtl number and ellipse axis ratio) the effect of the material parameters of the micropolar fluid are also considered. These parameters are the vortex viscosity, micro-inertia density and spin gradient viscosity. In comparison with Newtonian fluids, the study has shown that micropolar fluids display a clear reduction in heat transfer rate. The study shows also that the effect of vortex viscosity is the most significant material parameter on heat transfer rate.

Key-Words:- Micropolar – free convectioon – elliptic - tube – vortex viscosity - microrotation

1 Introduction

The theory of micropolar fluids has been proposed by Eringen [1]. In this theory the local effects arising from the microstructure and intrinsic motion of the fluid elements are taken into account. Such fluids can support surface and body couples which are not present in the theory of Newtonian fluids. Micropolar fluids are believed to be successful in describing the behavior of heterogeneous mixtures such as ferro liquids, colloidal fluids, animal blood , most slurries and some liquids with polymer additives. Eringen [2] developed the theory of thermo-micropolar fluids by extending the theory of micropolar fluids.

Previous studies of convective heat transfer in micropolar fluids have focused mainly on relatively simple geometry such as flat plates and circular cylinders. Refs. [3-8] are only examples. Most of these studies were mainly based on the numerical solution of simplified (boundary layer) governing equations. There were only a few attempts to investigate the case of natural convection from an elliptic cylinder placed in a micropolar fluid. Among these attempts were those made by Bhattacharyya and Pop [9] and Mahfouz [10]. Bhattacharyya and Pop solved the boundary layer equations to investigate the steady natural convection from an isothermal elliptic tube with its major axis either horizontal or vertical. They presented results for local Nusselt number along with velocity and temperature fields. While Mahfouz solved the full governing equation without boundary layer simplifications to investigate the transient natural convection from an isothermal elliptic tube with its major axis horizontal.

The main objective of this work is to study the effect of Rayliegh number and material parameters on natural convection from an isothermal elliptic tube placed in micropolar fluid with its major axis vertical. The buoyancy driven flow is assumed to be laminar and two dimensional.

Nomenclature

a	length of semi-major axis
Ar	axis ratio (=b/a)
b	length of semi-minor axis
c	dimensionless focal distance ($=\sqrt{1-Ar^2}$)
F_b	buoyancy force
K_v	vortex viscosity
j	micro-inertia density
Nu	local Nusselt number
$\overline{Nu}$	average Nusselt number
x', y'	Cartesian coordinates
Y^*	distance along minor axis $(=\frac{y'-b}{a}Ra^{0.25})$

Greek symbols

α	thermal diffusivity
β	coefficient of thermal expansion
γ	spin gradient viscosity
η, ξ	elliptical coordinates
μ	viscosity coefficient.
ν	kinematics viscosity

Subscripts

s,o at cylinder surface
∞ at infinite distance from the surface

2 Problem Formulation

Fig. 1 shows the physical model and coordinates system, consisting of an isothermal horizontal elliptic tube of infinite length placed with its major axis vertical in a quiescent micropolar fluid at temperature T_∞. The effect of temperature variation on fluid properties is considered negligible except for the buoyancy force term in the momentum equation (Boussinesqu approximation) . The conservation equations of mass, linear momentum , angular momentum and energy in terms of the vorticity, stream function, microrotation and temperature read the following:

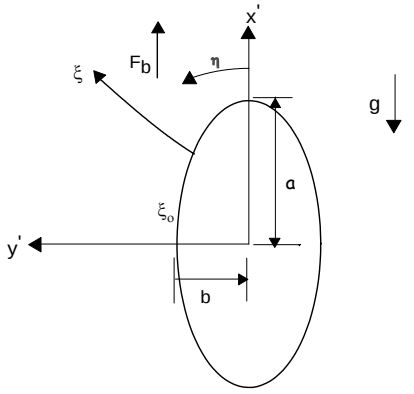

Fig. 1. Physical model and coordinate system

$$\frac{\partial \zeta'}{\partial \tau}+\frac{\partial \psi}{\partial y'}\frac{\partial \zeta'}{\partial x'}-\frac{\partial \psi}{\partial x'}\frac{\partial \zeta'}{\partial y'}=(\nu+\frac{K_v}{\rho})\nabla^2\zeta' - \frac{K_v}{\rho}\nabla^2\omega+\frac{1}{\rho}\left[\frac{\partial F_{y'}}{\partial x'}-\frac{\partial F_{x'}}{\partial y'}\right] \quad (1)$$

$$\zeta'+\nabla^2\psi'=0 \quad (2)$$

$$\frac{\partial \omega}{\partial \tau}+\frac{\partial \psi'}{\partial y'}\frac{\partial \omega}{\partial x'}-\frac{\partial \psi'}{\partial x'}\frac{\partial \omega}{\partial y'}=\frac{\gamma}{\rho j}\nabla^2\omega + \frac{K_v}{\rho j}(\zeta'-2\omega) \quad (3)$$

$$\frac{\partial T}{\partial \tau}+\frac{\partial \psi'}{\partial y'}\frac{\partial T}{\partial x'}-\frac{\partial \psi'}{\partial x'}\frac{\partial T}{\partial y'}=\frac{k}{\rho c_v}\nabla^2 T \quad (4)$$

where $\nabla^2=\frac{\partial^2}{\partial x'^2}+\frac{\partial^2}{\partial y'^2}$

τ is the time, ρ is the density, ν is the kinematic viscosity, k is the thermal conductivity and c_v is the specific heat. K_v, j and ϒ are the vortex viscosity, micro-inertia density and spin-gradient viscosity. ζ' is the vorticity, ψ' is the stream function, T is the temperature and ω is the component of microrotation vector whose direction of rotation is in the x′-y′ plane. $F_{x'}=\rho g\beta(T-T_\infty)$ *and* $F_{y'}=0$ are the components of the buoyancy force , where β is the coefficient of thermal expansion of the fluid.

The boundary conditions are mainly the no-slip, impermeability and no-spin conditions on the tube surface and the stagnant ambient conditions very far away from it.

-on the tube surface

$$\psi'=\frac{\partial \psi'}{\partial x'}=0\,,\ \frac{\partial \psi'}{\partial y'}=0\,,\ T=T_s \text{ and } \omega=0\ . \quad (5a)$$

-far away from the tube surface

$$\frac{\partial \psi'}{\partial x'}\to 0,\ \frac{\partial \psi'}{\partial y'}\to 0\,,\ T=T_\infty \text{ and } \omega\to 0 \quad (5b)$$

Now it is more convenient to use the following dimensionless variables:

$$x=\frac{x'}{a},\ y=\frac{y'}{a},\ t=\frac{\tau\alpha}{a^2},\ \psi=\frac{\psi'}{\alpha},\ \zeta=-\zeta'\frac{a^2}{\alpha},$$

$$M=\frac{a^2\omega}{\alpha},\quad \Delta=\frac{K_v}{\mu},\quad J=\frac{j}{a^2},\quad \lambda=\frac{\gamma}{j\mu}$$

and $\phi=\frac{T-T_\infty}{T_s-T_\infty}$

Using elliptic coordinates ξ,η such that $x=c\cosh(\xi)\cos(\eta)$, $y=c\sin sh(\xi)\sin(\eta)$, Eqs. (1)-(4) can now be written in terms of the above dimensionless variables as : .

$$D\frac{\partial \zeta}{\partial t}=\Pr(1+\Delta)\nabla^2\zeta+\frac{\partial \psi}{\partial \xi}\frac{\partial \zeta}{\partial \eta}-\frac{\partial \psi}{\partial \eta}\frac{\partial \zeta}{\partial \xi}+\Pr\ \Delta\nabla^2 M + (c/8)Ra\Pr\left[\cosh\xi\sin\eta\frac{\partial \phi}{\partial \xi}+\sinh\xi\ \cos\eta\frac{\partial \phi}{\partial \eta}\right] \quad (6)$$

$$D\zeta+\nabla^2\psi=0 \quad (7)$$

$$D\frac{\partial M}{\partial t}=\frac{\partial \psi}{\partial \xi}\frac{\partial M}{\partial \eta}-\frac{\partial \psi}{\partial \eta}\frac{\partial M}{\partial \eta}+\Pr\ \lambda\ \nabla^2 M - D\Pr\Delta(\zeta+2M)/J \quad (8)$$

$$D\frac{\partial \phi}{\partial t}=\nabla^2\phi+\frac{\partial \psi}{\partial \xi}\frac{\partial \phi}{\partial \eta}-\frac{\partial \psi}{\partial \eta}\frac{\partial \phi}{\partial \xi} \quad (9)$$

where $D=c^2(\cosh^2\xi-\cos^2\eta)$ is the Jacobian of transformation matrix, $Ra=g\beta(2a)^3(T_s-T_\infty)/\nu\alpha$ is the Rayleigh number and $\Pr=\nu/\alpha$ is the Prandtl number. The boundary conditions Eq. (5) can now be expressed as:

-on the tube surface ($\xi=\xi_o$), $\psi=\frac{\partial \psi}{\partial \xi}=0$,

$$\frac{\partial \psi}{\partial \eta}=0\,,\ \text{M = 0 and } \phi=1 \quad (10a)$$

and very far away from the tube surface ($\xi \to \infty$),

$$\frac{\partial \psi}{\partial \xi} \to 0, \quad \frac{\partial \psi}{\partial \eta} \to 0, \quad \mathrm{M} \to 0 \quad \text{and} \quad \phi \to 0 \qquad (10b)$$

where ξ_o defines the ellipse surface (= $\tanh^{-1}$Ar)

The temperature of the stagnant fluid around the tube at times t < 0 is T_∞ ($\phi = 0$) which is the same as that of the tube surface. At the start of computations ($t = 0$) the tube surface assumes a sudden temperature increase from T_∞ to T_s ($\phi = 1$), and from that moment the time development of both flow and thermal fields commences.

3 Method of Solution

The method used for solving the governing equations (6)-(9) to obtain the time development of both velocity and temperature fields is based on approximating the stream function, vorticity, microrotation and temperature using Fourier series expansion. The approach is similar to that used by Badr and Dennis [11]. The stream function ψ, vorticity ζ, microrotation Γ and temperature ϕ are now approximated as

$$\psi = \sum_{n=1}^{N} f_n \sin(n\eta) \qquad \text{n=1, 2,. N} \qquad (11a)$$

$$\zeta = \sum_{n=1}^{N} g_n \sin(n\eta) \qquad (11b)$$

$$M = \sum_{n=1}^{N} r_n \sin(n\eta) \qquad (11c)$$

$$\phi = H_o + \sum_{n=1}^{N} H_n \cos(n\eta) \qquad (11d)$$

where N is the number of terms in the Fourier series. The functions f_n, g_n, r_n, H_o and H_n are Fourier coefficients and all are dependent on ξ and t. The rest of the details of the method of solution is similar to that in Mahfouz [10] and Badr [11] and will not be repeated for the sake of brevity.

The local Nusselt number is defined as

$$Nu = 2ah/k \qquad (12)$$

where h is the local heat transfer coefficient defined as

$$h = \dot{q}/(T_o - T_\infty), \qquad \dot{q} = -k(\partial T/\partial s_n)_{\xi_o}$$

$\dot{q}$ is the rate of heat transfer per unit area , S_n is the normal direction to the tube surface. From the above definitions the Nu can be expressed in terms of Fourier coefficients H_0 and H_n as

$$Nu = \frac{-1}{\sqrt{D_o}}\left[\frac{\partial H_0}{\partial \xi} + 2\sum_{n=1}^{n=N}\frac{\partial H_n}{\partial \xi}\cos n\eta\right]_{\xi=\xi_o} \qquad (13)$$

The average Nusselt number can be expressed as

$$\overline{Nu} = \frac{1}{P}\int_0^P Nu \, dP = -\frac{2\pi a}{P}\left(\frac{\partial H_0}{\partial \xi}\right)_{\xi=\xi_o} \qquad (14)$$

where P is the perimeter of the elliptic section.

4 Results and Discussion

The governing equations along with the boundary conditions were solved in order to get the details of both flow and thermal fields. The simulations were carried out only after validating the method of solution by comparing the present results for the case of Newtonian fluids ($\Delta = 0$) with the most relevant results in the literature. Some of these comparisons are given in Mahfouz [8,10].

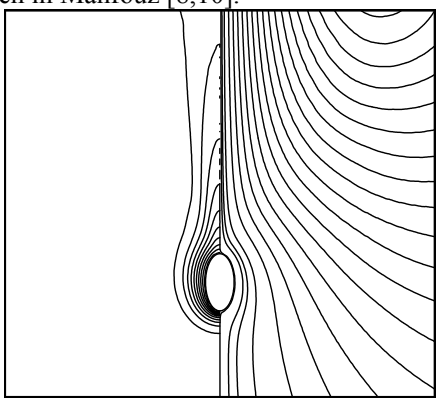

Fig 2 Steady patterns of streamlines (right) and isotherms (left)

The main controlling parameters are Rayleigh number Ra, Prandtl number Pr, axis ratio Ar and the material parameters λ, Δ and J. For the sake of brevity only the effect of Ra, Δ and J are considered while Pr, λ and Ar are fixed at 7, 1, 0.5 respectively. The Rayleigh number Ra, is considered in its moderate range up to 10^4. The material parameter Δ, which characterizes vortex viscosity is considered in the range from 0 to 10 while the material parameter J, which characterizes micro-inertia density, is considered in the range from 0.1 to 10. These values for material parameters satisfy the thermodynamics restrictions given by Eringen [2].

The time development of both flow and thermal fields is more or less similar to that of Newtonian fluids. That is immediately after the temperature of the tube surface is raised, a temperature gradient is established within the fluid layer adjacent to the tube surface, causing predomination of conduction mode of heat transfer. At this early time stages the newborn buoyancy force causes the commencement of fluid motion. As the time goes, the buoyancy–induced motion intensifies with gradual transition to convection mode domination heat transfer. At late

times, the convection mode dominates and the flow and thermal fields in the vicinity of the tube surface gradually tend to be almost steady. The steadiness in the nearby flow and thermal fields at late time leads to steady rates of heat transfer. A typical example for such flow and thermal fields at late time is shown in Fig. 2. The figure shows the flow field, in terms of streamlines, and the thermal field, in terms of isotherms, for the case of Ra=1000, $\lambda = 1$, $\Delta = 1$ and J=1. Since these fields are symmetrical about the vertical axis, only one half of each field is considered. The figure shows that these distributions are generally similar to those for Newtonian fluids.

Table 1 Effect of Ra and material parameters Δ and J on steady state average Nusselt number .

Ar	Ra	Δ	J	$\overline{Nu}$
0.5	10^3	------	------	4.03
		1	0.1	3.66
		5	0.1	3.23
		10	0.1	2.98
		1	1	3.63
		5	1	3.11
		10	1	2.87
		1	10	3.65
		5	10	3.08
		10	10	2.78
	10^4	-----	------	6.55
		1	0.1	5.79
		5	0.1	4.93
		10	0.1	4.56
		1	1	5.77
		5	1	4.79
		10	1	4.38
		1	10	5.79
		5	10	4.81
		10	10	4.35

------ refers to a Newtonian fluid

Table 1 shows the effect of Rayleigh number Ra, and the material parameters Δ and J of micropolar fluid on the steady state average Nusselt number, $\overline{Nu}$. It can be seen that the effect of Ra on steady state $\overline{Nu}$ is quite clear, that is at any fixed value of fluid material parameters as Ra increases the $\overline{Nu}$ increases. This is expected since increasing of Ra leads to increasing of convection currents and so increasing the heat transfer rate. Also, it can be seen that as the material parameter Δ increases at any fixed value of Ra the $\overline{Nu}$ decreases. The table also shows that at fixed values of Ra, and Δ the material parameter J has almost negligible effects on the $\overline{Nu}$ in the range considered for the parameters.

Fig. 3 shows the time variation of averaged Nusselt number $\overline{Nu}$, for the case of Ra=1000 , and at different values of dimensionless vortex viscosity Δ = 0, 1, 2, 5. The figure clearly shows that the general variation of $\overline{Nu}$ is similar to that for Newtonian fluids (Δ = 0). That is $\overline{Nu}$ evolves in a sequence of pure conductive, transient convective and steady convective processes. The pure conductive process prevails immediately after the tube surface temperature is increased. The high temperature gradient established near the tube surface results in high heat flux and so high values of $\overline{Nu}$. In this early time stages and as a result of quick developing of thermal boundary layer a quick decrease in $\overline{Nu}$ occurs, reaching to a minimum value at a certain short time. Beyond this time, the buoyancy force becomes more effective, causing transient convective process. This transition as shown in the figure takes a form of overshoot in $\overline{Nu}$. At late times the convective process gradually prevails with steady rates of heat transfer and so steady $\overline{Nu}$ gradually approach.

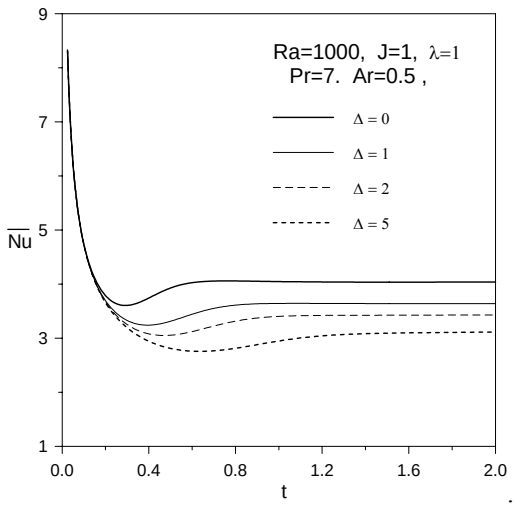

Fig. 3 The time development of $\overline{Nu}$

The figure also shows that the steady heat transfer rates (i.e steady $\overline{Nu}$) in the case of micropolar fluids (Δ =1, 2, 5) is lower than that for Newtonian fluid (Δ = 0). This decrease may be attributed, as explained in Hsu et al. [7], to the increase of the flow viscosity as a result of vortex viscosity. Increasing of flow viscosity weakens the flow convection currents and increases the thickness of the thermal boundary layer which in turn decreases heat

transfer rates (and so $\overline{Nu}$). Since the conduction mode of heat transfer is predominant in the initial stages the vortex viscosity has no effect and the heat transfer rates for micropolar fluid and that Newtonian fluid are identical. As the convection domination mode starts developing the vortex viscosity of micropolar fluid enhances the flow viscosity and so decreases the heat transfer rate. The larger the value of Δ the larger the flow viscosity and the lower the value of steady state $\overline{Nu}$.

The steady state local Nusselt number distributions at Ra =1000 and at different values of dimensionless vortex viscosity are shown in Fig. 4. Since the thermal field is symmetrical about the vertical axis, only one-half of Nu distribution is shown. It can be seen that at the topmost point on the tube surface ($\eta = 0$) the Nu is minimum for all values of Δ though it is slightly smaller for bigger values of Δ . As η increases from topmost point toward the bottommost point, the Nu slightly increases up to almost point ($\eta = 30$), and .keeps almost constant up to point ($\eta = 90$) then increases rapidly, reaching maximum at the bottommost point ($\eta = 180$). The figure clearly shows that, at any surface point Nu decreases as Δ increases. Decreasing of Nu on the tube surface as Δ increases explains the decrease of steady state $\overline{Nu}$ as Δ increases as shown in Table 1. and Fig. 3

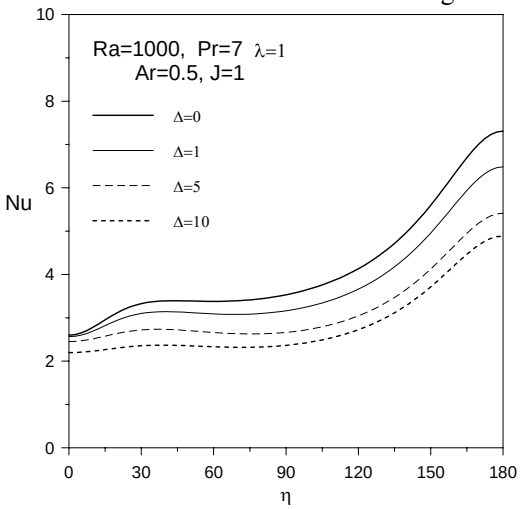

Fig. 4 Steady state local Nusselt number distibution

.

Fig. 5 shows the surface vorticity distribution for the same case. The surface vorticity at any fixed value of Δ increases rapidly from zero at topmost point ($\eta = 0$) to maximum at almost $\eta = 30$ then slightly decreases as η increases till almost $\eta = 120$ and then sharply decreases to zero at bottommost point. The figure also shows that as Δ increase the surface vorticity decreases at all points of the tube surface . Decreasing of surface vorticity reflects the decrease of velocity gradients at the tube surface which reflects in turn the weakness in the flow convection currents. The weaker the flow currents the smaller the heat transfer rates.

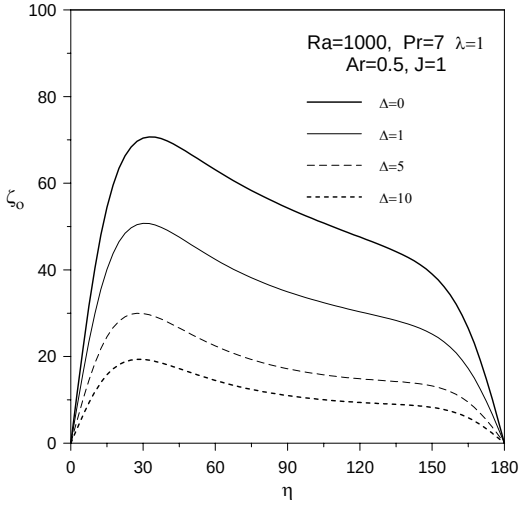

Fig. 5 Steady state surface vorticity distibution

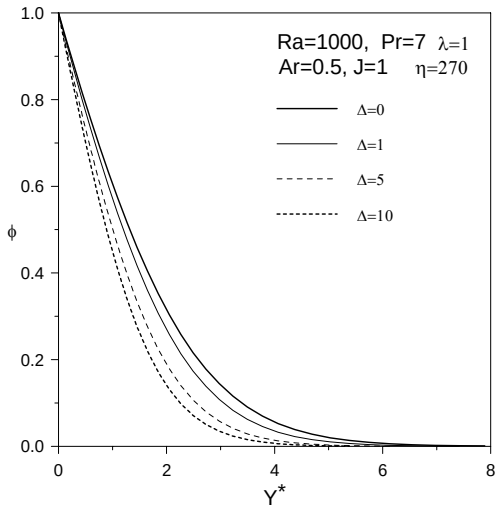

Fig. 6 Temperature variation along minor axis of the tube

Fig. 6 shows the temperature variation along the extension of the ellipse minor axis ($\eta = 270$) for the case of Ra = 1000, J=1 and at different values of dimensionless vortex viscosity, Δ . It can be seen that the fluid temperature decays with distance from tube surface till it reaches eventually the stagnant fluid temperature (i.e $\phi = 0$). Also. the figure clearly shows that as Δ increases the temperature gradient at the tube surface decreases and accordingly local heat transfer decreases which in turn means a decrease in Nu as can be seen in Fig.4.

Fig. 7 shows the variation of both vorticity and microrotation along the minor axis of the tube for the case of Ra=1000, J=1 and Δ=10. The figure shows that the values of both vorticity and microrotation are significant in the nearby region of the tube (in the boundary layer region) and almost negligible elsewhere along the axis extension . It can also be inferred that the direction of rotation of both mean flow and fluid elements along the minor axis is the same. The mean flow rotation is represented by vorticity while fluid elements rotation is represented by the microrotation. Moreover, the point of zero vorticity and zero microrotation or the point at which the mean flow and fluid elements change direction of rotaion is the same for both of them. The consisitency of this result with the logical exepectation from one side supports the valdity of the micropolar fluid model developed by Eringin [1] and from the other side supports the validaty and accuracy of the present numerical technique.

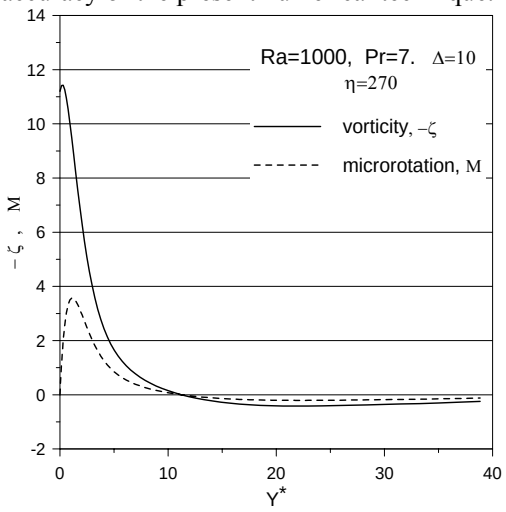

Fig.7. The vorticity and microrotation variation along minor axis

5 Conclusion

The effect of material parameters of micropolar fluid and Rayleigh number on natural heat convection from an isothermal elliptic tube and placed horizontally with its major axis vertical in a micropolar fluid was investigated. The study considered a range for Ra up to 10^4, a range for material parameter, Δ from 1 to 10 and a range for material parameter, J from 0.1 to 10. While the material parameter, λ Prandtl number and axis ratio are kept unchanged at 1, 7 and 0.5 respectively. The study showed that at certain values for material parameters as Rayleigh number increases the local heat transfer rate increases at all points on the cylinder surface which in turn increases the average heat transfer rate. The study has also shown that the vortex viscosity is the most important material parameter. A noticeable reduction in local and average heat transfer rates is observed as vortex viscosity increases. Generally, the study showed that the convective heat transfer rate decreases in the micropolar fluids in comparison with the Newtonian fluids.

References

[1] A. C Eringen, Simple micropolars, Int. J. Eng. Sci., 2, 1964, pp.205-217

[2] A. C. Eringen, Theory of thermomicrofluids, J. Math. Anal. Appl., 38, 1972 pp. 480-496.

[3] G. Ahmadi, Self-Similar solution of incompressible micropolar boundary layer flow over a semi-infinite plate, Int. J. Eng. Sci., 14, 1976, pp. 639-646.

[4] I. A. Hassanien, Mixed convection in micropolar boundary layer flow over a horizontal semi-infinite plate, ASME, J. of Fluids Engineering, 118, 1996, pp.833-838

[5] R. S. R. Gorla, Axisymmetric thermal boundary layer of a micropolar fluid on a cylinder, Int. J. Eng. Sci., 23, 1995, pp. 401-407

[6] A. A. Mohammedien, R. S. R. Gorla, and I. A. Hassanien, Mixed convection in an axisymmetric stagnation flow of micropolar fluid on a vertical cylinder, Acta Mecanica, 114, 1996, pp. 139-149

[7] T. Hsu, P. Hsu and S. Tsai, Natural convection of micropolar fluids in an enclosure with heat sources, Int. J. Heat Mass Transfer, 40(17), 1997, pp. 4239-4249

[8] F. M. Mahfouz, Transient free convection from a horizontal cylinder placed in a micropolar fluid, Heat and Mass Transfer, 39, 2003, pp. 455-462

[9] S. Bhattacharyya and I. Pop, Free convection from cylinders of elliptic cross section in micropolar fluids, Int. J. Eng. Sci., 34, 1996, pp. 1301-1310

[10] F. M. Mahfouz, Natural convection from an elliptic tube with major axis horizontal and placed in a micropolar fluid, Int. J. Heat and Mass Transfer, 47(6-7), 2004, pp. 1413-1422.

[11] H. M. Badr, and S. C. R. Dennis, Time-dependent viscous flow past an impulsively started rotating and translating circular cylinder, J. Fluid Mechanics, 158, 1985, pp. 447-488

[12] H. M. Badr, Laminar natural convection from an elliptic tube with different orientations, ASME J. of Heat Transfer, 119, 1997, pp. 709-718